

Dissection of keratin dynamics: different contributions of the actin and microtubule systems

Stefan Wöll, Reinhard Windoffer, Rudolf E. Leube*

Department of Anatomy, Johannes Gutenberg University Mainz, Becherweg 13, D-55128 Mainz, Germany

Abstract

It has only recently been recognized that intermediate filaments (IFs) and their assembly intermediates are highly motile cytoskeletal components with cell-type- and isotype-specific characteristics. To elucidate the cell-type-independent contribution of actin filaments and microtubules to these motile properties, fluorescent epithelial IF keratin polypeptides were introduced into non-epithelial, adrenal cortex-derived SW13 cells. Time-lapse fluorescence microscopy of stably transfected SW13 cell lines synthesizing fluorescent human keratin 8 and 18 chimeras HK8-CFP and HK18-YFP revealed extended filament networks that are entirely composed of transgene products and exhibit the same dynamic features as keratin systems in epithelial cells. Detailed analyses identified two distinct types of keratin motility: (I) Slow ($\sim 0.23 \mu\text{m}/\text{min}$), inward-directed, continuous transport of keratin filament precursor particles from the plasma membrane towards the cell interior, which is most pronounced in lamellipodia. (II) Fast ($\sim 17 \mu\text{m}/\text{min}$), bidirectional and intermittent transport of keratin particles in axonal-type cell processes. Disruption of actin filaments inhibited type I motility while type II motility remained. Conversely, microtubule disruption inhibited transport mode II while mode I continued. Combining the two treatments resulted in a complete block of keratin motility. We therefore conclude that keratin motility relies both on intact actin filaments and microtubules and is not dependent on epithelium-specific cellular factors.

© 2004 Elsevier GmbH. All rights reserved.

Keywords: Live cell imaging; Green fluorescent protein; Nocodazole; Latrunculin; Cytoskeleton; Intermediate filament; Keratin; Actin; Tubulin

Introduction

The framework of the cytoplasmic cytoskeleton is composed of three major filament systems. They include the 2–5-nm actin-based microfilaments, the 25-nm microtubules that are composed of tubulin heterodimers, and the compositionally most diverse intermediate filaments (IFs) of 8–12 nm diameter. When considering the various functions that rely on the cytoskeleton, e.g., migration, cell division, vesicle trafficking, or stress

response, it appears imperative that the reactions of the cytoskeletal components are co-ordinated and that no part acts entirely on its own. In accordance, it was reported a long time ago that drugs that specifically disrupt either actin filaments or microtubules also affect the organization of the IF system (e.g., Celis et al., 1984; Goldman, 1971; Hynes and Destree, 1978; Osborn et al., 1980). Yet, other authors found that only microtubule but not actin disruption leads to IF reorganization (Gordon et al., 1978). To complicate the situation further, several groups did not detect any alterations in IF distribution in certain situations when either of the other cytoskeletal filament systems was destroyed and thus used this very property to define specific IF types

*Corresponding author. Tel.: +49 6131 392 2731;
fax: +49 6131 392 4615.

E-mail address: leube@uni-mainz.de (R.E. Leube).

(e.g., Knapp et al., 1983a,b; Osborn et al., 1977; Sun and Green, 1978) although the combined destruction of actin filaments and microtubules was accompanied by significant IF alterations (Knapp et al., 1983a,b). As a result, the variably occurring structural IF alterations, which—in contrast to the other cytoskeletal filament systems—did not lead to disassembly but rather to reorganization and formation of perinuclear filament bundles, may be attributed to specific properties of individual IF types in different cellular environments or could be interpreted as non-specific effects.

Recent years have provided overwhelming evidence that molecular ties exist between all cytoskeletal filaments. Static links are provided by the plakins, a complex family of large molecules that facilitate physical contact between different filament types, cell adhesion sites and cytoplasmic organelles (Fuchs and Karakesiosoglou, 2001; Leung et al., 2002). Probably the most prominent plakin is plectin, which acts as a general cytoskeletal cross-linker with multiple interaction types depending on the splice variants present in a given cell (Steinbock and Wiche, 1999; Wiche, 1998). In addition, dynamic attachments are established by motor proteins that enable IFs and their precursors to move in relation to the other cytoskeletal filaments (review in Helfand et al., 2003a).

Imaging of IFs in living cells has revealed that they are highly dynamic cell components both in terms of motility and turnover (recent reviews in Helfand et al., 2003a, 2004). This also includes the epithelial keratin IFs, which are essential stabilizers of the epithelial cytoskeleton by providing resilience to mechanical stress (Coulombe and Wong, 2004; Herrmann et al., 2003). Various types of motility have been described for keratin filaments (KFs) and keratin particles by several groups (Liovic et al., 2003; Werner et al., 2004; Windoffer et al., 2002, 2004; Windoffer and Leube, 1999, 2001, 2004; Yoon et al., 2001), and it has been shown that the dynamic keratin organization is modulated by cellular phosphorylation (Strnad et al., 2001, 2002, 2003).

To examine the importance of actin filaments and microtubules for the motile properties of keratin assemblies, we monitored the effects of actin filament and microtubule disruptions in living vulva carcinoma-derived A-431 cells producing fluorescent keratin 13 chimeras (Windoffer and Leube, 1999). We observed that adding of cytochalasin D resulted in network retraction leading to partial collapse of the extended KF system. On the other hand, treatment of the same cell line with nocodazole led to a marked decrease in KF network oscillations (see also Liovic et al., 2003; Yoon et al., 2001). Furthermore, we examined the effects of microtubule- and actin-disrupting drugs on the de novo formation of the KF cytoskeleton at the end of mitosis (Windoffer and Leube, 2001). Coincidentally, KFs are

completely disassembled into soluble subunits and granules at the beginning of mitosis in A-431 cells. This material is subsequently used for the rebuilding of a new KF network. Adding both cytochalasin D and nocodazole prevented formation of a typical KF network. In the presence of cytochalasin, elongated clumped material was formed that moved toward the cell center and lacked anchorage to the cell cortex. On the other hand, incubation with nocodazole resulted in restricted fluorescence enrichment in the cell periphery, and it seemed that granules dissolved into diffuse, possibly filamentous structures. Taken together, these results suggested that both actin filaments and microtubules are important for dynamic KF organization, yet in a different way that may not always be apparent in still pictures.

A dynamic interaction between microtubules and IFs has also been recognized for neurofilaments, peripherin and vimentin (Chan et al., 2003; Helfand et al., 2002, 2003b; Martys et al., 1999; Prahlad et al., 1998, 2000; Shah et al., 2000; Yabe et al., 1999, 2000, 2001; Yoon et al., 2001). It has been pointed out, however, especially in direct comparisons between keratin and vimentin IFs, that significant differences exist with respect to dynamic properties and transport specificities (Yoon et al., 2001).

To further define principal aspects of the interrelationship of the IF cytoskeleton with microtubules and actin filaments in a cell-type-independent context with improved technology, we decided to study the behavior of keratin IF proteins in SW13 cells, that usually lack IF proteins altogether (Hedberg and Chen, 1986). By adding drugs that selectively inactivate actin filaments or microtubules, the contribution of each system to the dynamic behavior of KFs and KF precursors was determined in SW13 cells that were stably transfected with cDNAs coding for chimeric keratin-fluorescent protein pairs.

Materials and methods

cDNA cloning

For construction of HK8ΔT-EGFP, a ~1.3-kb EcoRI/SacI fragment was excised from HCK8-containing human keratin 8 cDNA in vector pDs5 (Hofmann and Franke, 1997). The EcoRI site was blunted and the fragment subcloned into SmaI/SacI-cleaved vector pSP64 (Promega, Madison, WI), thereby generating plasmid pHK8ΔT. The ~1.3-kb keratin 8 cDNA fragment was excised from this plasmid with BamHI/EcoRI and inserted into BglII/EcoRI-cleaved vector pEGFP-N3 (Clontech, Palo Alto, CA). The encoded polypeptide consists of human keratin 8 (lacking its 59 carboxyterminal amino acids) that is connected to

enhanced green fluorescent protein (GFP) by the linker sequence NSAVDGTAGPGSIAT.

Establishment of stably transfected cell lines

Human small-cell carcinoma SW13 cells derived from the adrenal cortex (ATCC CCL-105) were trypsinized, seeded at high density on 60 mm diameter culture dishes (Greiner Bio-One, Frickenhausen, Germany), and grown under the conditions specified by ATCC. Cells were transfected at near-confluency (90%) with cDNA constructs using Lipofectamine 2000 reagent (Invitrogen, Karlsruhe, Germany). 500 μ l OPTI-MEM (Invitrogen) were mixed with 15 μ l Lipofectamine 2000 in one 1.5-ml reaction tube. In another tube 4 μ g HK18-YFP1 (Strnad et al., 2002) and 4 μ g of the plasmid encoding HK8-CFP (Windoffer et al., 2004) were added to 500 μ l OPTI-MEM. Both tubes were incubated at room temperature for 5 min prior to mixing and further incubation at room temperature for another 20 min. The solution was then added dropwise to the culture dish containing 4 ml high glucose DMEM (PAA Laboratories, Cölbe, Germany) supplemented with 10% fetal calf serum (PAA Laboratories). After 24 h incubation at 37 °C and 5% CO₂, cells were evenly distributed on two 10-cm diameter culture dishes. After another 24 h, 1100 μ g/ml geneticin and 1% penicillin/streptomycin stock solution (10,000 U penicillin/ml, 10 mg/ml streptomycin) were added to the culture medium (all reagents from Invitrogen). Cells were maintained in this medium until single cell clones could be identified that were picked and expanded in single wells of a 24-well plate. To assure the clonal character of the established cell lines, cells were again seeded at low density and individual clones were repicked into 24-well plates.

Fluorescence microscopy of fixed cells

For indirect immunofluorescence microscopy, cultured cells were grown on glass coverslips, fixed with methanol (precooled to –20 °C) for 5 min and treated for 10 s with acetone (also precooled to –20 °C). Incubation with murine monoclonal antibodies against α -tubulin (1:300 dilution; Amersham Biosciences, Freiburg, Germany) lasted for 60–90 min at room temperature. It was followed by three washes with PBS for 5 min each and incubation with cy3-conjugated goat anti-mouse antibodies (1:700 dilution; Rockland, Gilbertsville, PA) for 30–45 min. After several washes with PBS, slides were mounted in Elvanol (1 g Mowiol 4-88 [Calbiochem GmbH, Frankfurt, Germany] in 4 ml distilled water and 2 ml glycerol).

For detection of actin, cells were fixed as described above and then incubated for 30–45 min with Texas-

Red-coupled phalloidin (1:50 in PBS; Molecular Probes, Eugene, OR). After several washes with PBS, slides were mounted in Elvanol.

Drug treatment

Cells were treated for 15, 25, 30, 35, 45, 60, and 70 min with 30 μ M latrunculin B (Sigma), for 30, 45, 60, and 150 min with 30, 40, 60, and 100 μ M nocodazole (Sigma), or for 15, 25 and 45 min with both drugs (30 μ M latrunculin B, 40 μ M nocodazole). Cells were fixed, and cytoskeletal filament distribution was analyzed by fluorescence microscopy to determine appropriate conditions for live cell imaging.

Live cell imaging

For time-lapse fluorescence microscopy of living cells, epifluorescence using inverse optics (Olympus, Hamburg, Germany) was recorded with an IMAGO slow scan CCD camera (TILL Photonics, Gräfelfing, Germany) as described previously (Windoffer et al., 2002, 2004; Windoffer and Leube, 2001, 2004). Cells grown in a glass bottom-equipped Petri dish (Mattek, Ashland, MA) with phenol-red-free Hanks' medium (Invitrogen) were placed on the microscope stage that was engulfed by a climate chamber (37 °C). Fluorescence excitation with monochromatic light was accomplished with a monochromator. Images were imported into Image-Pro Plus 4.5 (MediaCybernetics, Silver Spring, MD) and converted into movies (MPEG-1). The position of cell borders was determined from transmitted light images that were recorded in parallel.

Measurement of transport rates

To determine transport rates of particles, pictures recorded at different time points were merged. Single fluorescent particles were marked and the positional difference between both images was measured using Adobe Photoshop 8 (Adobe Systems Incorporated). The speed of fragment movement was calculated taking into account the traveled distance, the microscope magnification and the time interval between the recorded pictures. The average speed and the standard error of the mean (SEM) were calculated and combined in comparative histograms.

Preparation of cytoskeletal extracts, gel electrophoresis and immunoblotting

IF-containing cell fractions were prepared by standard methods (Achtstaetter et al., 1986). Polypeptides contained in high-salt-resistant pellets were separated by 10% SDS-PAGE and stained with Coomassie Brilliant

Blue (Serva, Heidelberg, Germany), or individual polypeptides were identified after immunoblotting with specific rabbit-anti-GFP antibodies (Molecular Probes), followed by horseradish peroxidase-coupled secondary goat anti-rabbit antibodies (Dianova, Hamburg, Germany) and detection with an enhanced chemiluminescence system (Amersham Biosciences). Co-electrophoresed size marker SDS-6H was purchased from Sigma.

Results

In vivo assembly of keratin-fluorescent protein hybrids in non-epithelial SW13 cells into extended keratin filament networks

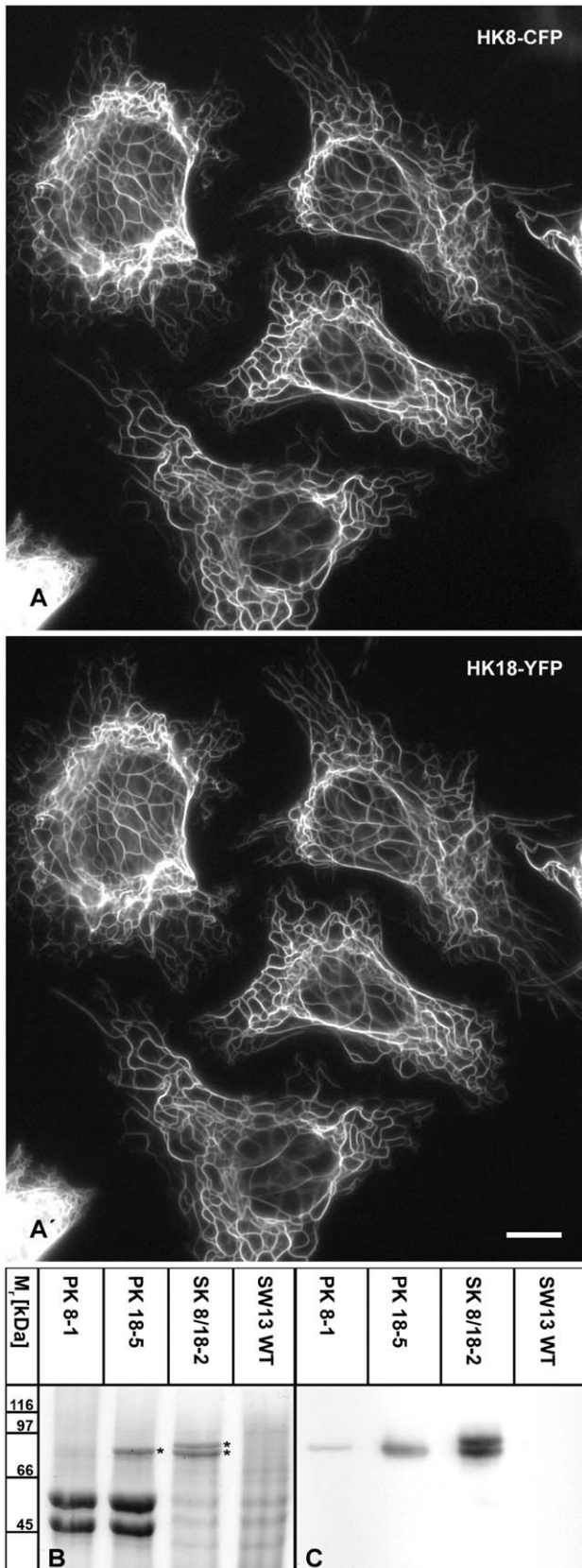
We have previously observed that transfected fluorescent keratin polypeptides form characteristic cytoplasmic networks in non-epithelial, adrenal cortex-derived SW13 cells (Windoffer et al., 2004; see also Yoon et al., 2001) which are devoid of any cytoplasmic IF (Hedberg and Chen, 1986). To further study properties and characteristics of these ectopic networks that are entirely composed of hybrid polypeptides, we established clonal cell lines producing keratin 8 and 18 chimeras HK8-CFP and HK18-YFP. One such cell line, SK8/18-2, was examined in further detail. Extended KF networks were detectable in all cells by fluorescence microscopy (Fig. 1A and A'). As expected for the obligatory keratin heteropolymers, CFP- and YFP-fluorescence patterns were virtually indistinguishable (compare Fig. 1A and Fig. 1A'), although CFP-dependent fluorescence was weaker due to the reduced quantum yield of this fluorophore. Furthermore, both polypeptide types were enriched in high salt-resistant cytoskeletal cell fractions in which they could be detected by Coomassie Blue staining as major components (Fig. 1B) and by immunoblotting using antibodies either against GFP (Fig. 1C) or keratins (not shown). Significant amounts of wild-type keratins were neither detected in wild-type SW13 cells nor in SK8/18-2 cells (Fig. 1B and data not shown).

Detection of two types of keratin particle movement in SW13 cells synthesizing fluorescent keratin filament networks

Time-lapse fluorescence images were recorded to analyze the dynamic properties of the exogenous KF network in SK8/18-2 cells. The resulting movies showed that the entire network was in constant slow motion as has been described for various epithelial cell lines producing fluorescent keratin polypeptides (Liovic et al., 2003; Windoffer and Leube, 1999; Yoon et al.,

2001). The most pronounced motility was noted in the cell periphery, where keratin particles were abundant and clearly detectable (Fig. 2A; compare with Windoffer et al., 2004). It has been shown previously that these particles are KF precursors that participate in the cell cortex-determined continuous turnover of the KF system and its de novo formation (Windoffer and Leube, 2001; Windoffer et al., 2004). The particles originated in close proximity to the plasma membrane as small spheroids that enlarged and elongated into rodlets until they integrated into the peripheral network (movie 1; see also stills in Fig. 2A). They moved continuously toward the cell center at an average speed of $\sim 232.4 \pm 25$ nm/min ($n = 10$). The centripetal movement continued after network integration albeit at a reduced speed of $\sim 89.8 \pm 6$ nm/min ($n = 17$). Particles were particularly abundant in lamellipodia, that were frequently formed. In these, initially KF-free cytoplasmic extensions multiple particles appeared rapidly within a few minutes. The newly generated fluorescent structures also became first visible close to the plasma membrane, elongated into rodlets, and were transported toward the peripheral KF network into which they integrated (Fig. 2B; movie 2). The transport in lamellipodia was unidirectional and directed toward the cell center with a continuous speed of $\sim 229.0 \pm 15$ nm/min ($n = 14$) which is almost identical to the inward movement recorded in other peripheral cellular domains (see above). Particles in lamellipodia, however, were often oriented perpendicular to the plasma membrane and not in parallel as was observed in regions of minor cell ruffling (compare Fig. 2A and B). Furthermore, in contrast to inactive peripheral regions, the frequency of particle generation was considerably increased in lamellipodia.

Occasionally, cells were noted that presented extremely long processes reminiscent of axonal-type extensions. One such cell is shown in Fig. 3 which, in addition to multiple lamellipodia, contained a single process of over 0.3 mm. This process had an equal diameter of ~ 1.5 μ m throughout its length with multiple dynamic microspike-like protrusions and a growth cone-like enlargement at its most distal tip. Several fluorescent keratin particles were detected in this enormous cytoplasmic extension. The motility of these filamentous particles was analyzed by time-lapse fluorescence imaging (movie 3). Most particles were stationary with only minor oscillatory movements for extended periods of time (up to an hour or even longer). After these intervals rapid movement was noted, that was almost two orders of magnitude faster than the continuous, inward-directed motility observed in lamellipodia and peripheral cytoplasmic regions. Most particles moved toward the cell body although some were also transported away from it. The average speed was 19.36 ± 1.6 μ m/min ($n = 4$) for anterograde transport and 16.914 ± 0.8 μ m/min ($n = 2$) for retrograde transport, both of which are most likely



underestimates given the comparatively long recording intervals of 25 s.

Keratin particle movement in the presence of nocodazole is slow, inward-directed and continuous

Since the analyses of keratin particle movement in SK8/18-2 cells suggested the presence of a fast and a slow type of motility, each with distinct features, we wanted to determine the importance of microtubules for either type of motility and wished to find out whether microtubule-independent factors are also involved. To achieve these goals, cells were treated with nocodazole to disrupt microtubules. Adding the drug resulted in complete disassembly of microtubules and concurrent rearrangement of the KF network (Fig. 4). While the majority of KFs concentrated around the nucleus within 45 min, several KFs remained extended toward the cell periphery most of which co-aligned with newly formed actin stress fibers (Fig. 4B, B' and B''; compare also with Osborn et al., 1980). In time-lapse fluorescence analyses the KF rearrangement was shown to be caused by collapse and retraction of the network toward the nucleus (Fig. 5; movie 4). Remarkably, continuation of particle formation was observed in the remaining cytoplasmic extensions. These particles, however, were not stationary but moved continuously inward at a speed of 239.2 ± 21.4 nm/min ($n = 12$). This value is very similar to that determined for peripheral particles in lamellipodia and in other areas of the cytoplasmic

Fig. 1. Detection of fluorescent keratin hybrids HK8-CFP and HK18-YFP in SW13-derived, stably transfected cell line SK8/18-2. (A,A') Double fluorescence microscopy of methanol/acetone-fixed SK8/18-2 cells detecting HK8-CFP (A) and HK18-YFP (A'). Note that both fluorescent polypeptides co-distribute completely within the extended cytoplasmic filament networks in all cells (bar, 10 μ m). (B,C) Coomassie-brilliant blue staining (B) and immunoblot analysis (C) of polypeptides that were enriched in cytoskeletal fractions from different cell lines and separated by 10% SDS polyacrylamide gel electrophoresis. Cytoskeletal extracts were prepared from SK8/18-2 cells, non-transfected SW13 cells (SW13WT), hepatocellular carcinoma-derived PLC subline PK8-1 synthesizing a truncated version of keratin 8 fused to EGFP (chimera HK8 Δ T-EGFP), and PLC subline PK18-5 producing HK18-YFP hybrids. Note that the hybrid polypeptides are detectable in the cytoskeletal fractions of transfected cells either by Coomassie-Brilliant Blue staining (asterisks in (B), except for HK8 Δ T-EGFP in PK8-1) or by immunoblotting using anti-GFP antibodies (C). In addition, abundant amounts of wild-type keratin polypeptides 8 and 18 are visible in the Coomassie-stained gel (lanes PK 8-1 and PK 18-5), whereas only non-coinciding, non-IF background bands are present in SK8/18-2 and SW13WT cells. The position and M_r of co-electrophoresed size markers are given at the left margin.

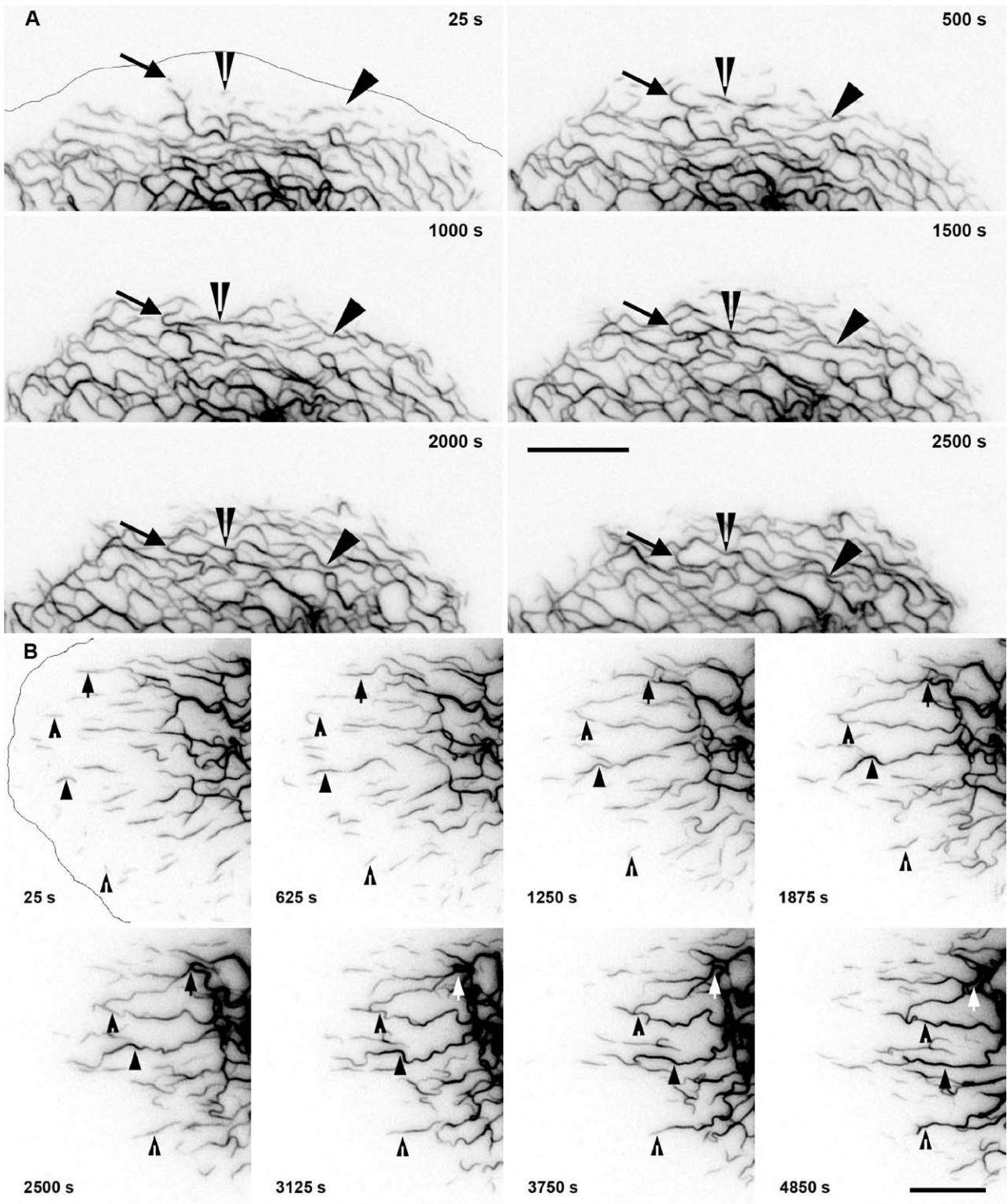


Fig. 2. Fluorescence micrographs (inverse presentation) of peripheral regions of living SK8/18-2 cells taken from time-lapse recordings detecting dynamics of HK18-YFP distribution. The complete time series are provided as movies 1 and 2 corresponding to (A) and (B), respectively (recording intervals, 25 s). (A) Cell region close to the plasma membrane (line at time point 25 s) where fluorescent keratin particles originate, enlarge, elongate and incorporate into the peripheral KF network. (B) Keratin particles in a lamellipodium. Note that small particles are also generated in close proximity to the plasma membrane (line at time point 25 s), elongate, fuse during transport toward the cell interior and integrate into the peripheral KF system. In both instances particle transport exceeds the inward movement of the network but all processes are continuous and directed toward the cell interior (arrows highlight a few particles before and after network integration). Bars, 10 μ m.

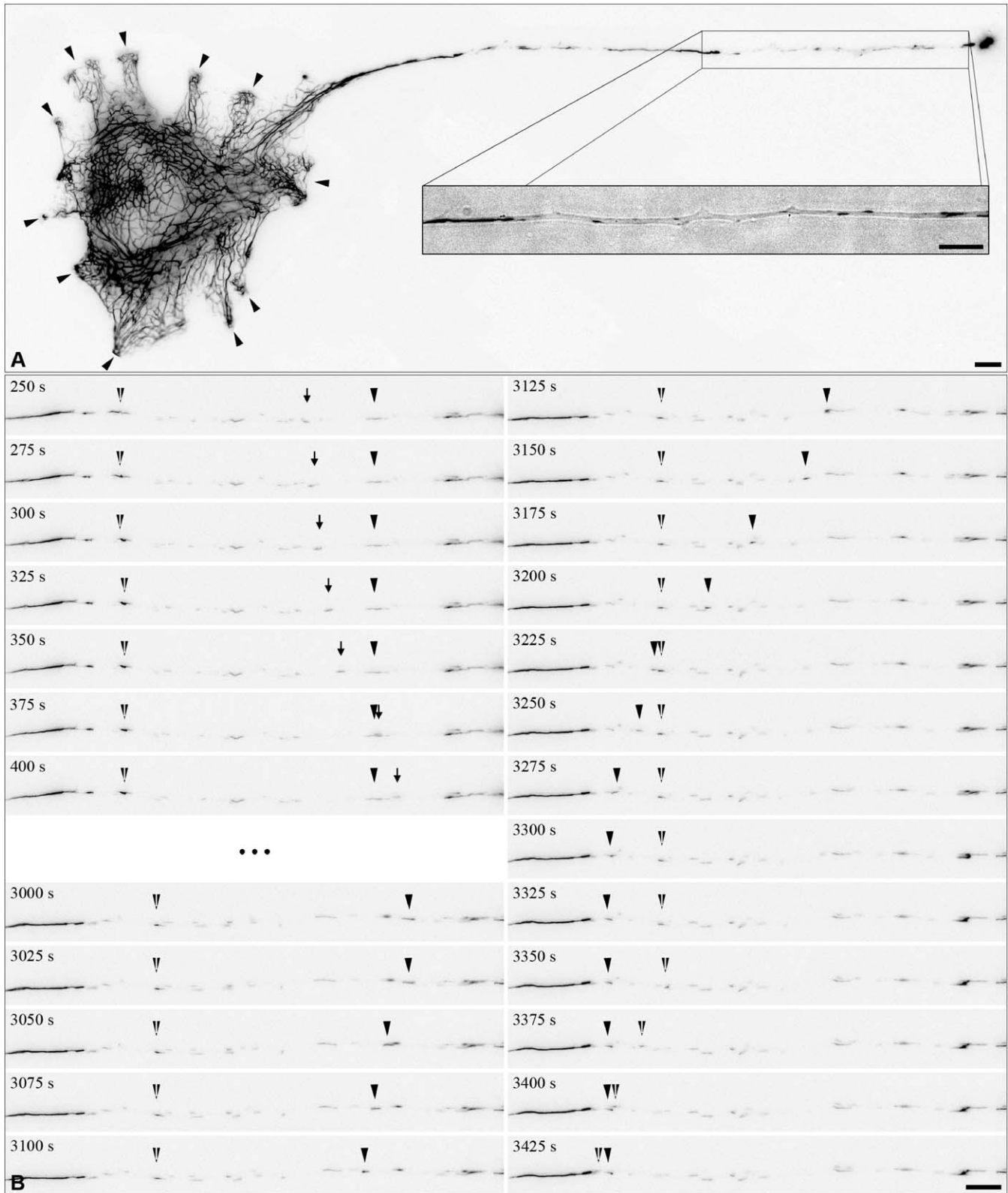


Fig. 3. Fluorescence microscopy (inverse presentation; montage of multiple images) of single live SK8/18-2 cell detecting HK18-YFP chimeras. Note the extensive fluorescently labelled network in the perinuclear cytoplasm, multiple lamellipodia (arrowheads) and a very long axonal-like cytoplasmic extension toward the right in (A), a part of which is shown as a superimposed image combining fluorescence and interference contrast pictures in the inset. Fluorescence recordings of this part were done at 25 s intervals to produce movie 3. Examples of particle movement within the elongated cytoplasmic extension are highlighted by arrows in (B) revealing long periods of minor motility that are interrupted by short periods of rapid movement either toward the cell body (arrowheads) or toward the cell periphery (arrow). Bars, 10 μm .

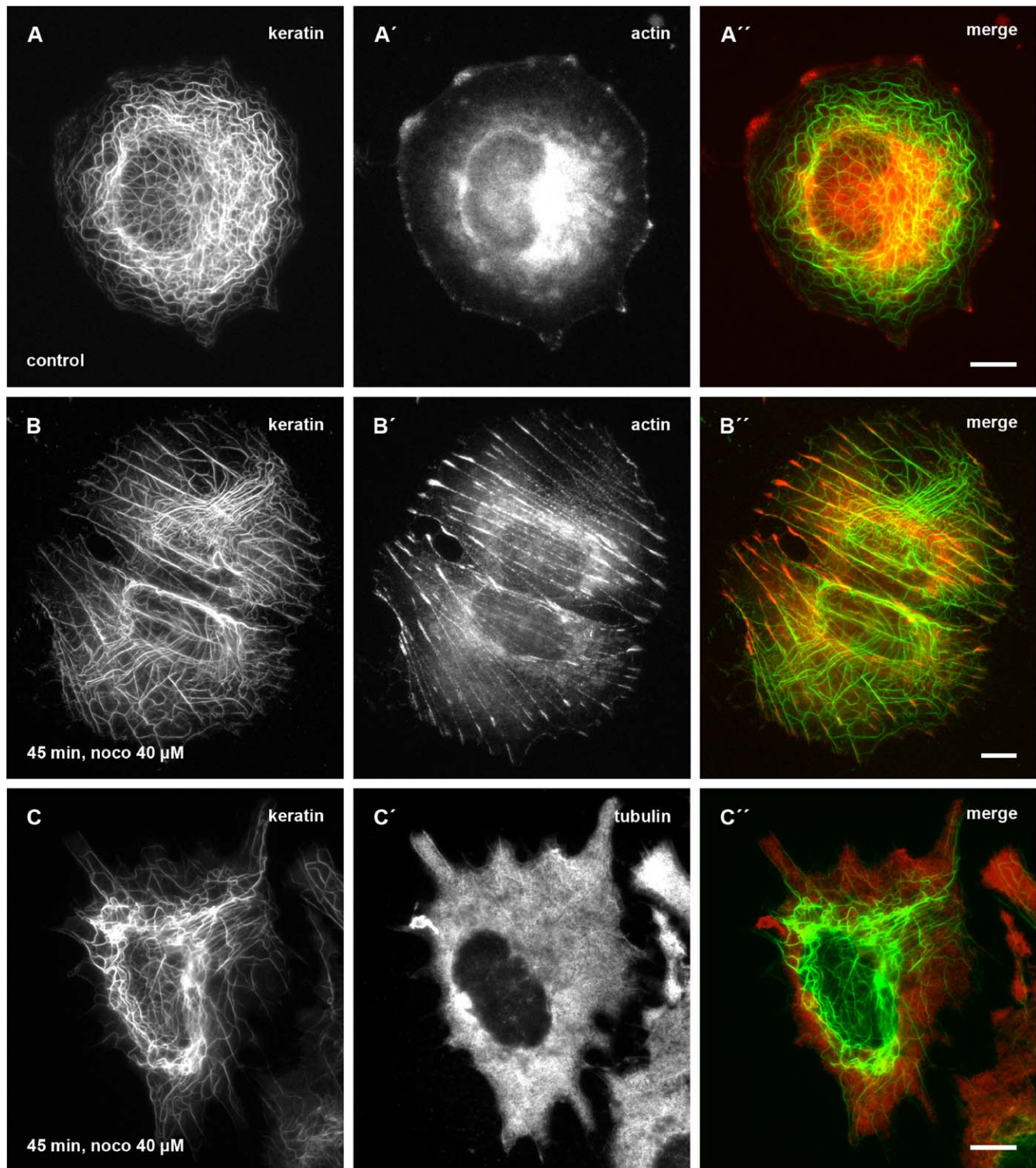


Fig. 4. Double fluorescence microscopy of methanol/acetone-fixed SK8/18-2 cells either under standard conditions (control) or after incubation with 40 μM nocodazole (noco) for 45 min detecting HK18-YFP chimeras (keratin; A,B,C) together with actin using Texas-Red-coupled phalloidin (actin; A',B') or tubulin using monoclonal anti- α tubulin antibodies in combination with cy3-coupled secondary antibodies (tubulin; C'). The superimposed recordings are shown in color (keratin in green; actin and tubulin in red) in the panel at right (merge; A'',B'',C''). Note the co-alignment of KFs and actin fibers in the presence of nocodazole (B''). Bars, 10 μm.

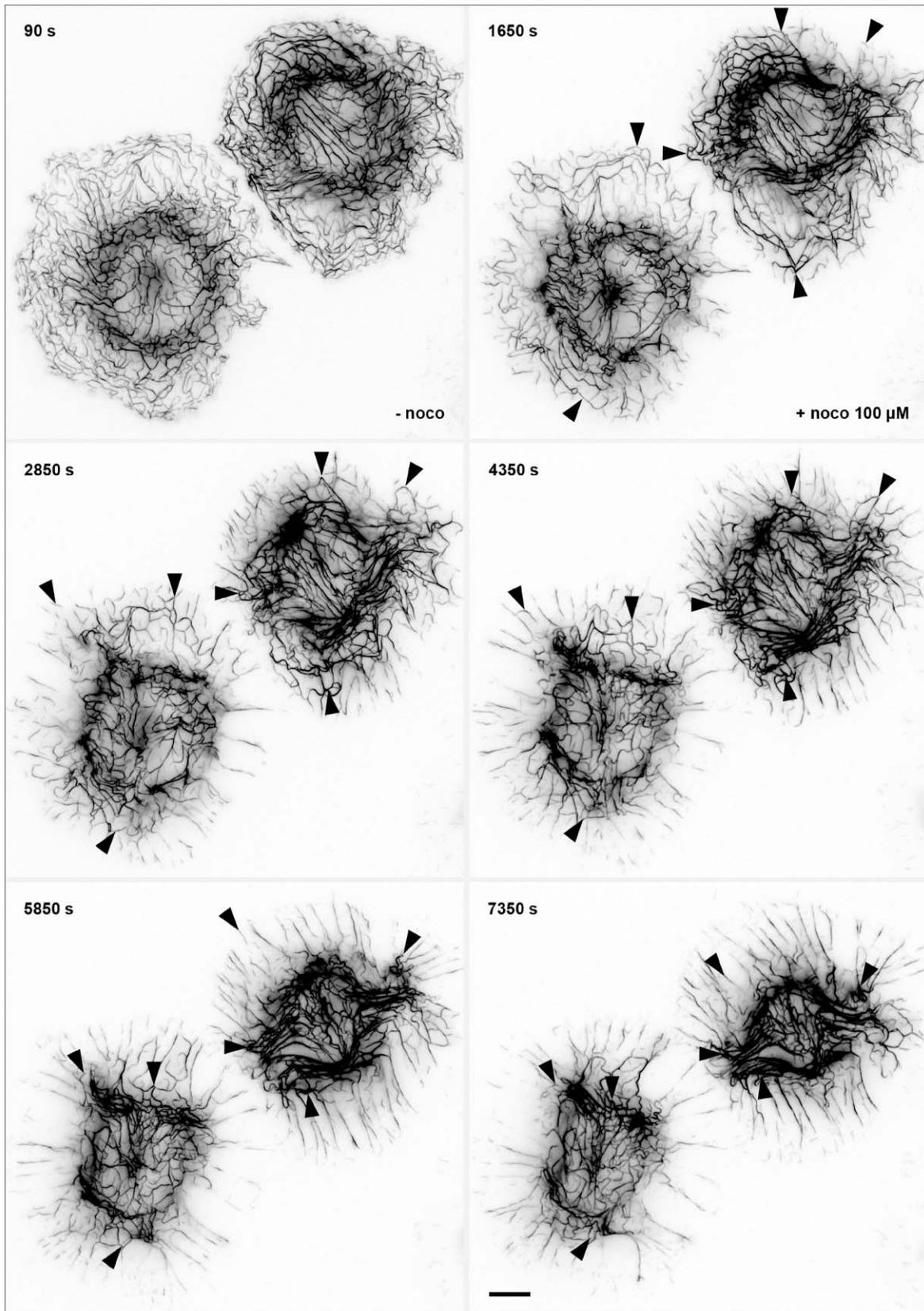


Fig. 5. Time-lapse fluorescence micrographs (inverse presentation) detecting HK18-YFP in SK8/18-2 cells immediately before addition of nocodazole (– noco) and at various time points after addition of 100 μM nocodazole at time point 300 s (+ noco). The complete time series is presented as movie 4 (recording intervals 30 s). Note the continuously ongoing inward movement of material from the cell periphery toward the cell interior (examples highlighted by arrowheads). Bar, 10 μm.

periphery of untreated control cells (Fig. 2; movies 1 and 2). The fluorescent particles still integrated into the condensed KF network. Rapid, discontinuous motility of particles was not detected anymore in the presence of nocodazole.

Keratin particle movement in the presence of latrunculin B is fast, bidirectional and discontinuous

To determine whether the comparatively slow, unidirectional, continuous, and microtubule-independent keratin particle motility relies on an intact actin system and, conversely, to examine which type of particle movement is detectable in the absence of actin filaments, SK8/18-2 cells were treated with the actin-disrupting agent latrunculin B. Drug concentrations were such that the actin filament system was completely destroyed while microtubules remained intact (Fig. 6B' and C'). The cells contracted after latrunculin B application, and KFs concentrated in dense bundles around the nucleus (Fig. 6B). At later stages, numerous keratin particles were seen in the peripheral cytoplasm some of which appeared as rings (Fig. 6C) suggesting that keratin particle formation did not cease. To analyze keratin dynamics in the presence of latrunculin B, time-lapse fluorescence recordings were prepared (Fig. 7; movies 5 and 6). In this way, intermittently moving keratin particles were clearly delineated in the flat peripheral cytoplasm after collapse of the KF network. Long stationary periods alternated with short intervals of fast transport. During the transport phase, particle speed was measured to be $15.77 \pm 2.7 \mu\text{m}/\text{min}$ ($n = 12$) and occurred along distinct tracks. Although the majority of particles was transported toward the perinuclear region, some were also transported in the opposite direction (e.g., split arrowhead in Fig. 7B). The particles were highly flexible. They fused, forming rings on occasion, and retained the capacity of network integration. The continuous, inward-directed slow type of particle transport was almost completely abrogated in the presence of latrunculin B.

Inactivation of the actin and microtubule systems completely inhibits keratin motility

Finally, to examine whether the microtubule and actin systems together account for all keratin particle motility and how the combined treatment affects the organization and dynamics of the KF network, SK8/18-2 cells were treated with latrunculin B and nocodazole either simultaneously (Fig. 8) or in succession (Fig. 9; movies 5 and 6). As expected, the combined application of both drugs led to a perinuclear collapse of the KF network with only residual filaments extending toward the cell periphery. Remarkably, these peripheral

filaments remained in association with areas of tubulin fluorescence (Fig. 8) as if physical contact between both persisted. The fluorescence time-lapse recording shown in movie 7 (Fig. 9A) confirmed that keratin particles, which were still formed in the presence of latrunculin B, were transported rapidly and intermittently along tracks in the peripheral cytoplasm. Subsequent addition of nocodazole prevented all types of motility. In addition, particle formation was not detected in significant amounts anymore although particles remained fusion-competent. Conversely, when cells were first treated with nocodazole (movie 8; Fig. 9B), particle formation continued in the cell periphery and slow continuous inward transport occurred. The end point, i.e., the dynamic behavior of the keratin cytoskeleton in the presence of both drugs was similar to that seen when the drugs were applied in the reverse order.

Comparison of particle transport velocities reveals two types of motility

Average particle velocities that had been determined either in different cellular domains (peripheral subplasmalemmal region, lamellipodium, axonal-type extension) or in the presence of either latrunculin B or nocodazole were accumulated in a histogram (Fig. 10). Comparison of the transport values clearly established two distinct types of particle speed in untreated cells: a slow transport occurring in peripheral cellular domains and lamellipodia with a mean velocity of 231 nm/min and a fast transport occurring in the axonal-type process either antero- or retrogradely with mean velocities of 9.7 and 16.9 $\mu\text{m}/\text{min}$, respectively. Remarkably, the slow transport persisted in the presence of nocodazole (mean velocity of 239 nm/min) whereas the fast transport persisted in the presence of latrunculin B (mean velocity of 15.7 $\mu\text{m}/\text{min}$). We therefore conclude that the slow type of motility in the peripheral cytoplasm and lamellipodia is dependent on an intact actin filament system whereas the fast type of motility in axonal-like processes is determined by microtubules.

Discussion

By using live cell imaging, we readdressed a long-standing debate regarding the manner in which the actin and microtubule networks affect the organization of the keratin system. We obtained strong evidence that both are intricately interlaced with the dynamics of the keratin network and showed that each contributes to keratin motility in a different and highly specific way in a cell-type-independent fashion.

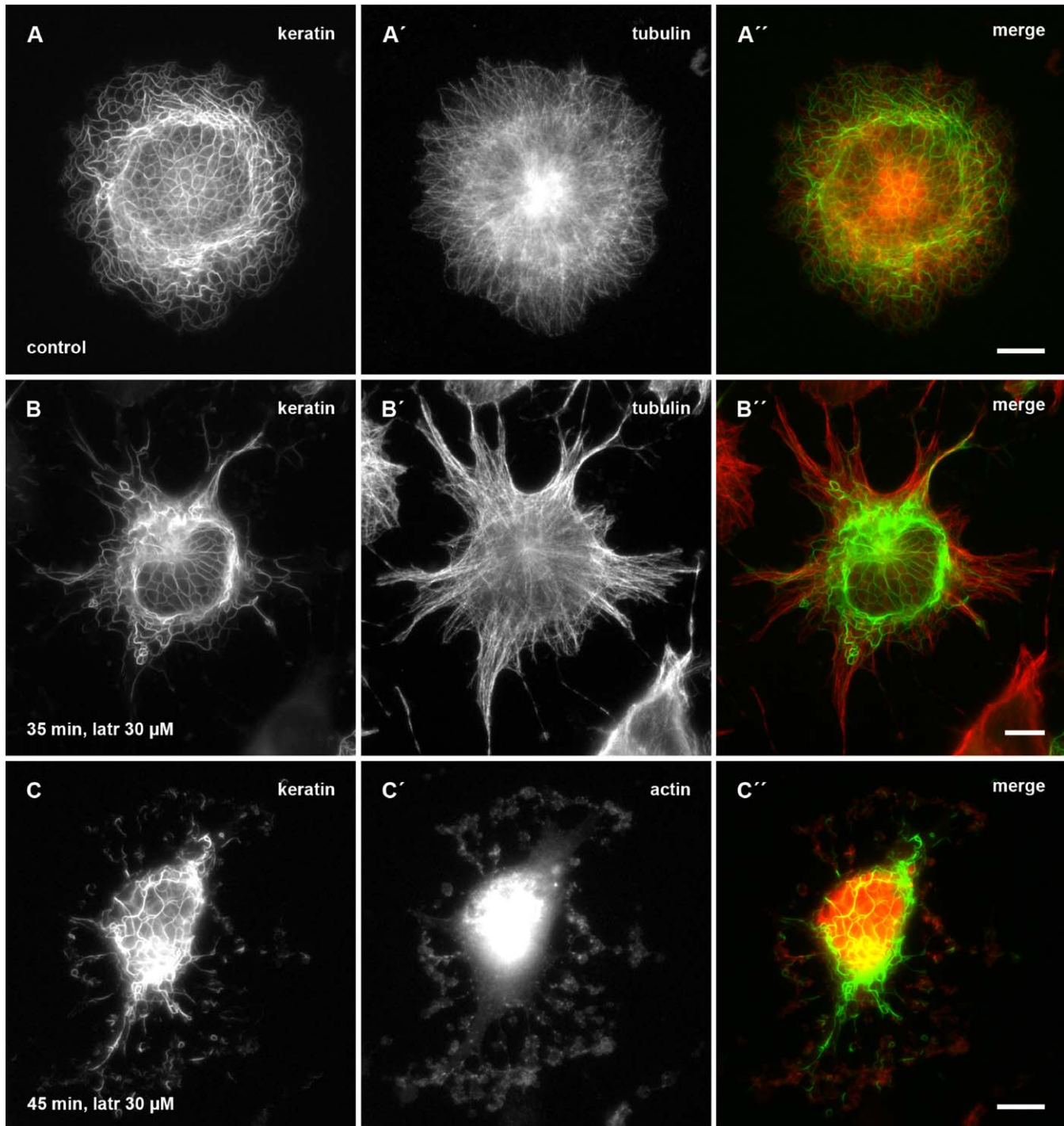
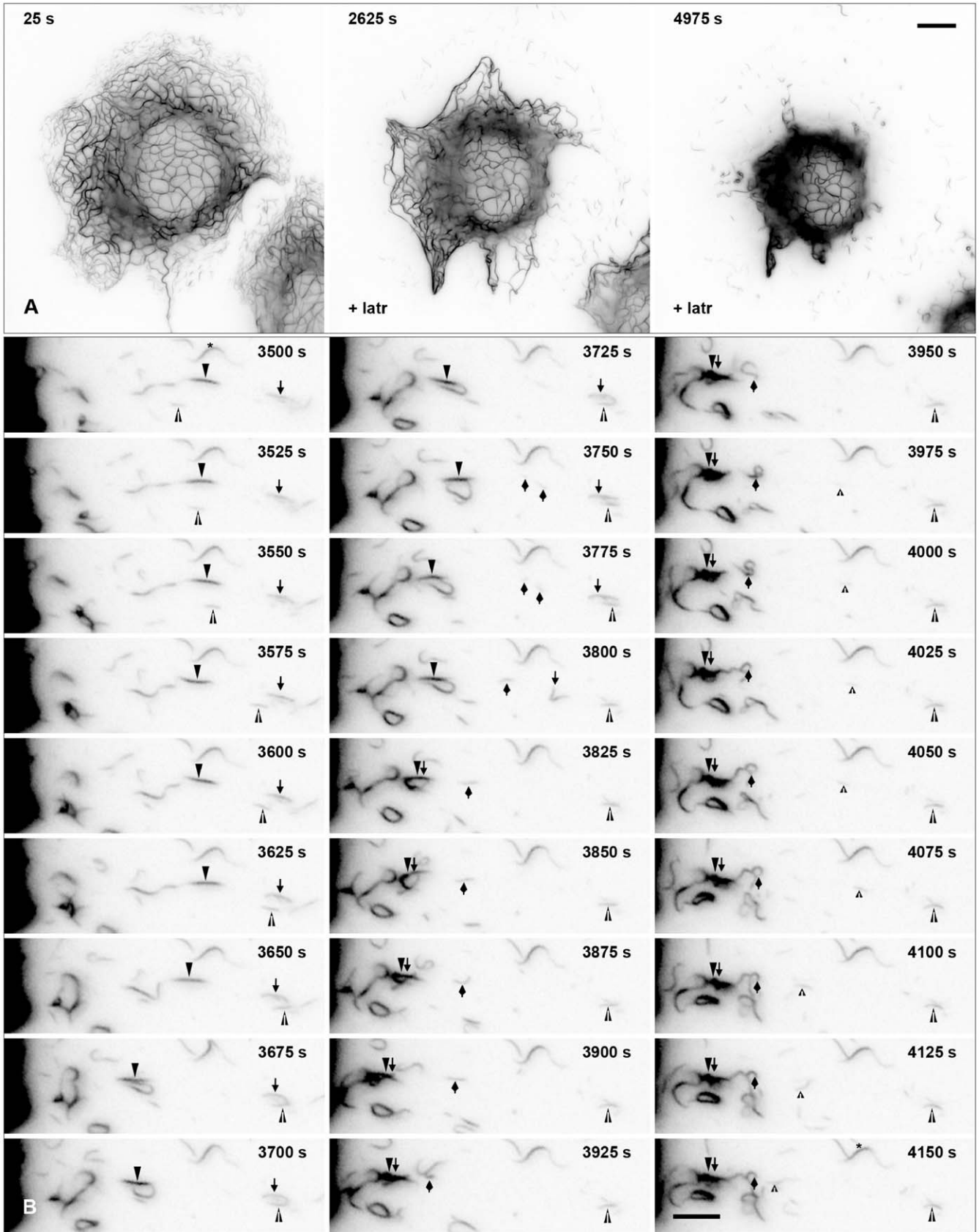


Fig. 6. Double fluorescence microscopy of methanol/acetone-fixed SK8/18-2 cells either under standard conditions (control) or after incubation with 30 μ M latrunculin B (latr) for either 35 or 45 min detecting HK18-YFP chimeras (keratin; A, B, C) together with tubulin using monoclonal anti- α tubulin antibodies in combination with cy3-coupled secondary antibodies (tubulin; A',B'), or actin using Texas-Red-coupled phalloidin (actin; C'). The superimposed recordings are shown in color (keratin in green; tubulin and actin in red) in the panel at right (merge; A'',B'',C''). Bars, 10 μ m.

Microtubule-based keratin motility

By analyzing transport of keratin particles in spontaneously occurring axonal-type cell processes and in cells

lacking a functional actin filament system, we identified microtubule-dependent keratin motility which most likely corresponds to that described for small keratin particles in epithelial cells (Liovic et al., 2003). The



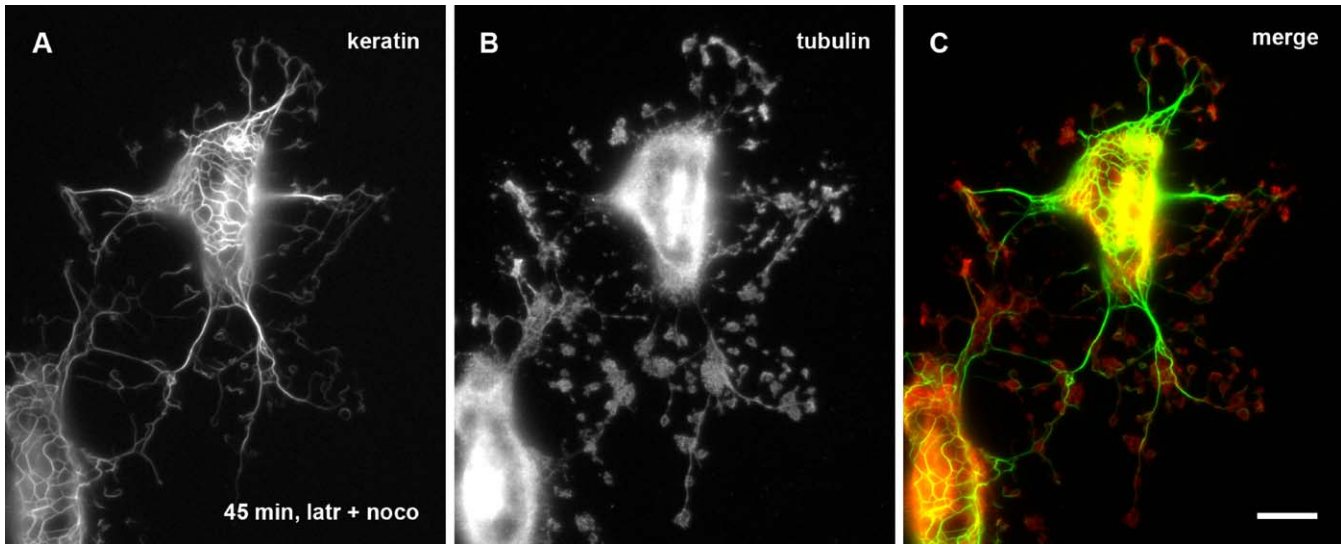


Fig. 8. Double fluorescence microscopy of methanol/acetone-fixed SK8/18-2 cells treated with 30 μM latrunculin B (latr) and 40 μM nocodazole (noco) for 45 min detecting HK18-YFP (keratin; (A)) together with tubulin ((B); monoclonal anti α -tubulin antibodies). The superimposed fluorescence images detecting keratin (green) and tubulin (red) are shown at right (merge). Note that remaining areas of tubulin fluorescence remain connected by keratin fibrils. Bar, 10 μm .

conclusion that this type of transport is determined by microtubules and their associated motor proteins is based on the following key findings: (i) The transport is rapid, ranging between 9.7 and 16.9 $\mu\text{m}/\text{min}$, which is in the same order of magnitude as transport velocities determined for microtubule-associated motors (for review Hirokawa, 1998) and rapidly transported IF particles (reviews in Helfand et al., 2004; Wang and Brown, 2001). (ii) It is discontinuous with alternating stationary periods and transport intervals, which is a well-known characteristic of microtubule-dependent transport of neurofilament and vimentin particles (Helfand et al., 2004; Roy et al., 2000; Wang and Brown, 2001; Wang et al., 2000; Yabe et al., 2001). (iii) It is bi-directional, occurring mostly in a direction toward the cell center, but also occasionally in the opposite direction, a property also shared by microtubule-dependent transport of particles composed of other IF polypeptides (Chan et al., 2003; Helfand et al., 2002, 2003a,b, 2004; Martys et al., 1999; Roy et al., 2000; Shah et al., 2000; Wang et al., 2000; Yoon et al., 1998). (iv) It is sensitive to nocodazole, as is also

the case for transport of various IFs in different cell types (Chan et al., 2003; Liovic et al., 2003; Martys et al., 1999; Prahlad et al., 1998; Yabe et al., 2001; Yoon et al., 2001). (v) It is insensitive to latrunculin treatment and becomes even more pronounced in the presence of actin filament-disrupting drugs (Figs. 7, 9 and movies 5–7; see also Yoon et al., 2001). Furthermore, strong evidence has been presented in other systems that this type of IF motility is accomplished by microtubule-associated motor proteins of the kinesin- and dynein-type which physically associate with IFs (Gyoeva and Gelfand, 1991; Helfand et al., 2002, 2003b; Kreitzer et al., 1999; Liao and Gundersen, 1998; Prahlad et al., 1998, 2000; Shah et al., 2000; Xia et al., 2003; Yabe et al., 1999, 2000; Yoon et al., 2001). Why Yoon et al. (2001) were not able to provide evidence for the contribution of dynein motors to keratin motility in cells expressing fluorescent keratin chimeras is not known. It is possible, however, that these authors detected remaining actin-dependent motility after dynein antibody injection, since particle speed was determined to be only $240 \pm 120 \text{ nm}/\text{min}$, a value close



Fig. 7. Time-lapse fluorescence recordings (inverse presentation) of HK18-YFP in SK8/18-2 cells before and after adding 30 μM latrunculin B at time point 1050 s (+latr). (A) Survey views showing the latrunculin-induced collapse of the KF network around the nucleus with remaining keratin particles in the peripheral cytoplasm. The complete time series is presented as movie 5 (recording intervals 25 s) revealing fast, intermittent and bidirectional transport of keratin particles. (B) High-magnification images taken from a peripheral region of the cell shown at bottom right in (A). Single particles are labeled by arrows demonstrating that they remain stationary most of the time and move rapidly during short intervals toward the remnant keratin bundles in the perinuclear region along a single track. One particle that is marked by a split arrowhead moves in the opposite direction away from the cell center along a neighboring track. The complete time series and surrounding areas of the cytoplasm containing multiple particles is provided as movie 6. Bars, 10 μm in (A); 5 μm in (B).

to the actin-dependent transport rate observed in the present study. Considering that microtubule-dependent transport is shared by all cytoplasmic IF types that have been studied to date in an *in vivo* context and that it is also detectable when IF polypeptides are expressed ectopically (this study), it can be concluded that the underlying molecular mechanisms are not restricted to a particular cell type but are basic cellular properties.

In addition to IF particle transport, microtubules may also regulate KF network motility, as we noted

previously that nocodazole incubation almost completely abolished KF oscillations in an epithelial cell line (Windoffer and Leube, 1999; see also Liovic et al., 2003), which cytochalasin did not in another system (Yoon et al., 2001). Similarly, KF motility was also reduced in nocodazole-treated SK8/18-2 cells. Perhaps, the antagonistic action of dynein and kinesin motors provides tensile strength for the KF system through multiple, transient interaction sites between microtubule-associated motor proteins and KFs. In support, microtubule destruction resulted in IF network collapse around the nucleus. Furthermore, the presence of residual KFs connecting areas of tubulin accumulation in nocodazole-treated cells (e.g., Fig. 8) can be taken as another indication of focal contact points between both cytoskeletal elements. Again, it appears that similar properties are also shared by the other IF polypeptides, although differences clearly exist (e.g., Yoon et al., 1998). Affinities between motor proteins and specific IF polypeptides, availability of motor proteins in particular cell types and interaction sites of individual IFs may vary considerably.

Actin-dependent keratin dynamics

Our experiments further provided strong evidence for actin-dependent transport of keratin particles. This transport is clearly distinguished from microtubule-dependent IF motility: it is almost two orders of magnitude slower, strictly unidirectional, continuous, insensitive to nocodazole, and sensitive to latrunculin B. This type of dynamic interaction between the actin and IF system has not been fully recognized so far and only very few earlier studies pointed to the existence of such a link, especially in cortical actin-rich regions (Correia et al., 1999; Gard et al., 1997; Gard and Klymkowsky, 1998; Tint et al., 1991). Given the comparatively slow speed of the observed actin-dependent transport and its continuously ongoing nature, it appears rather unlikely that it is directly driven by motor proteins, although an association between neurofilaments and myosin Va has

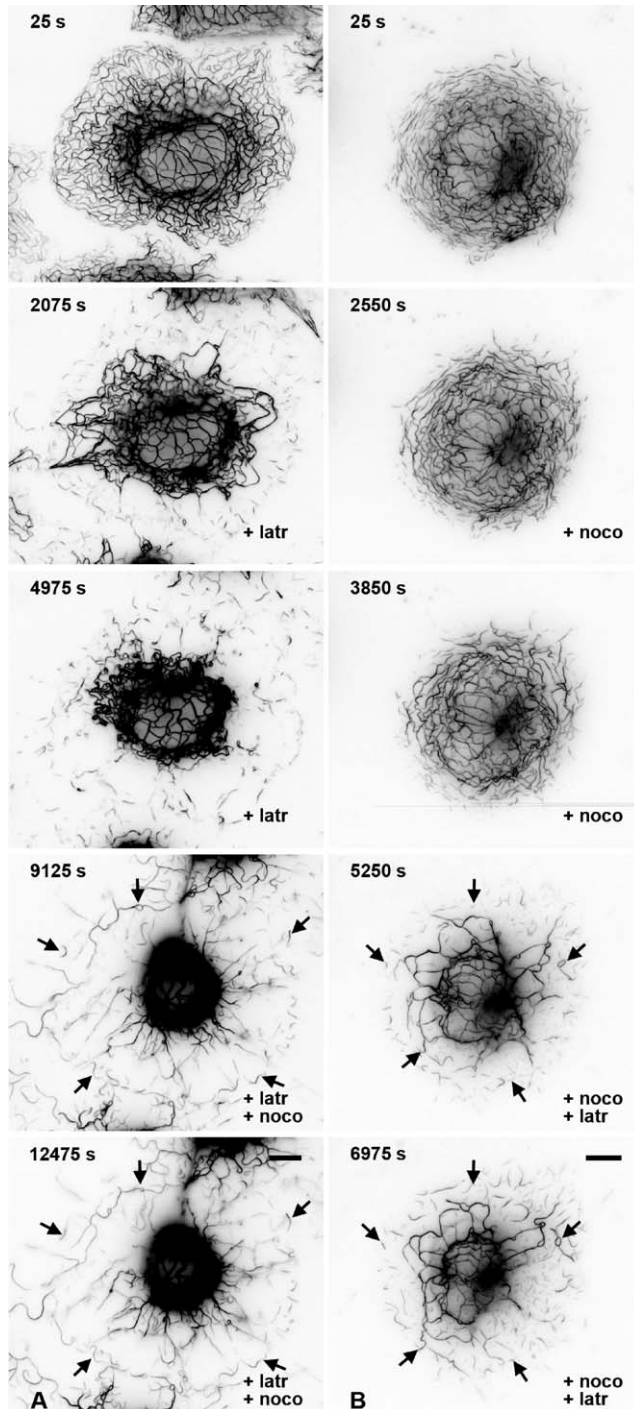


Fig. 9. Fluorescence micrographs taken from time-lapse image series depicting HK18-YFP fluorescence distribution patterns in SK8/18-2 cells that were either first treated with 30 μ M latrunculin (+ latr) for 3857 s (between time points 1125 and 3975 s) prior to addition of 40 μ M nocodazole at time point 5000 s ((A); noco; corresponding movie 7; recording intervals, 25 s) or, alternatively, first treated with 40 μ M nocodazole for 1500 s (between time points 2475 and 3975 s) before adding 30 μ M latrunculin at 3975 s ((B); corresponding to movie 8; recording intervals, 25 s). Note the differential cessation of motility of the keratin system upon application of the drugs, that is completely abolished in the presence of both drugs (see structures denoted by arrows). Bars, 10 μ m.

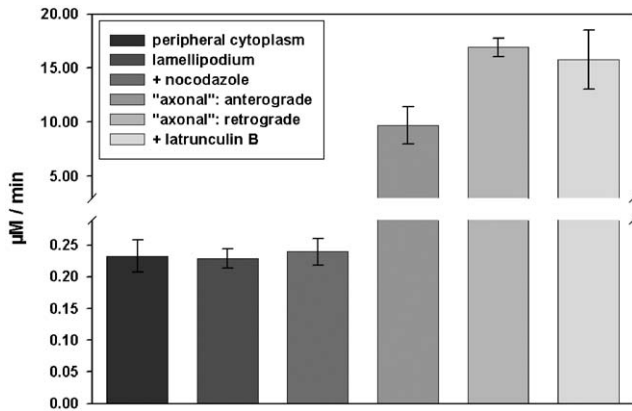


Fig. 10. Histogram presenting mean particle velocities together with the SEM measured in the peripheral cytoplasm ($n = 10$), in lamellipodia ($n = 14$), or in axon-like processes (either away from the perinuclear cytoplasm ($n = 4$; anterograde) or towards it ($n = 2$; retrograde)) in untreated cells or in cells that were either incubated with nocodazole or with latrunculin B. Note the two groups of particle speed that differ by up to two orders of magnitude.

been reported (Rao et al., 2002). A much more plausible alternative is that it is coupled to actin treadmilling/polymerization, plasma membrane protrusion and/or rearward flow occurring in lamellipodia and lamella which are of comparable speed, depending on the particular situation (Carlier, 1998; Fujiwara et al., 2002; Pollard and Borisy, 2003; Rottner et al., 1999; Waterman-Storer and Salmon, 1997). An interesting feature of actin-dependent keratin organization is that it is coupled to KF precursor formation and growth (Windoffer and Leube, 2001; Windoffer et al., 2004). Utilizing mechanisms that determine actin nucleation and polymerization for KF assembly would be a perfect means to determine cytoskeletal organization in a coordinated fashion. In support, Weber and Bement (2002) have provided *in vitro* evidence that F-actin serves as a platform for keratin organization, especially during initial phases of assembly. Inhibition of F-actin assembly in this system resulted in KF aggregate formation. The reported formation of adhesion-dependent fimbrin–vimentin complexes in macrophages can be taken as a further indication for such a mechanism of coordinated actin and IF formation. Regulation of these processes could be mediated by specific adhesion sites such as focal contacts that are formed in lamellipodia (Zaidel-Bar et al., 2003) and that have been observed at the tips of filopodia, where they function in adhesion zipper formation of epithelial sheets (e.g., Vasioukhin et al., 2000). A function of the actin system for transport of early keratin assembly intermediates was also observed in cells producing mutant fluorescent keratin chimeras (Werner et al., 2004). These mutants, that occur in

epidermolysis bullosa simplex patients, formed granules in the subplasmalemmal region that moved toward the cell interior at a speed of ~ 600 nm/min and enlarged until their rapid disassembly. Addition of latrunculin B but not of nocodazole inhibited the inward movement of these mutant keratin granules completely. Most remarkably, formation of small keratin particles ceased immediately, which, however, seems to be different from the situation encountered in SK8/18-2 cells.

Contribution of actin filaments and microtubules to KF network organization

Taking the observations on the actin- and microtubule-dependent transport and organization of the keratin cytoskeleton together, we deduce the following working model. Within the actin-rich cell cortex, assembly of KF precursors is initiated using the soluble and freely diffusible cytoplasmic keratin pool (Windoffer and Leube, 2001; Windoffer et al., 2004). Local conditions must exist in distinct microdomains within the cell cortex that favor keratin polymerization and are subject to regulation. Such yet to be identified factors must be tethered to the actin cytoskeleton and/or plasma membrane. Given the increase in keratin particle formation in lamellipodia, it is attractive to speculate that nascent focal adhesion sites not only affect actin polymerization but are also involved either directly or through some type of signaling mechanism in the regulation of KF precursor formation. Fluorescence microscopy of living cells co-expressing fluorescent keratins together with fluorescent actin and/or its associates will help to clarify the situation. Furthermore, by employing bleaching techniques it should be possible to determine whether an active transport model by motor proteins and/or a piggy back model of attached KF precursors is the basis for the observed inward transport of growing KF precursors. The highly flexible precursors remain polymerization competent in a way that they can further elongate, fuse with each other or even with themselves, and are capable of inserting into pre-existing “endless” KFs (see also Windoffer et al., 2004). At a certain, yet still poorly-defined point particles are delivered from the actin system to microtubules. Such a release mechanism has been observed *in vitro* (Weber and Bement, 2002) and may also exist *in vivo*, since mutant keratin particles have been described that lack the capacity to associate with microtubules *in vivo* and are only poorly integrated/assembled into a KF network (Werner et al., 2004). The restriction of these mutant polypeptide granular assemblies to the peripheral cytoplasm and their rapid disassembly within a distinct, localized zone can be taken as an indication that keratin particles are delivered to microtubules at

around this position and that this transition is important for integration into the KF network. As a consequence, microtubules are needed to spread the KF network throughout the cytoplasm by utilizing their associated opposing motors. These may also be important factors determining the tensile strength of the IF system.

We postulate that the basic mechanisms of coupling among the three major cytoskeletal filament systems are shared by all cells and that the dynamic interactions are attenuated to the needs of each specific cell type by the specific mix of factors and polypeptide isoforms present. A holistic view will require consideration of the entire cytoskeleton participating in the regulation of cell shape changes as they occur in all cells, either during development into differentiated tissues, during proliferation, or in regeneration or disease.

Acknowledgements

The expert technical assistance of Ursula Wilhelm is gratefully acknowledged. The work was supported in part by the German Research Council. The senior author wishes to express his gratitude to Professor Franke for instilling his enthusiasm for the endless and miraculous beauty of nature which provides many exciting answers and even more fascinating enigma.

Appendix A. Supplementary data

The online version of this article contains additional supplementary data. Please visit [doi:10.1016/j.ejcb.2004.12.004](https://doi.org/10.1016/j.ejcb.2004.12.004).

References

- Achtstaetter, T., Hatzfeld, M., Quinlan, R.A., Parmelee, D.C., Franke, W.W., 1986. Separation of cytokeratin polypeptides by gel electrophoretic and chromatographic techniques and their identification by immunoblotting. *Methods Enzymol.* 134, 355–371.
- Carlier, M.F., 1998. Control of actin dynamics. *Curr. Opin. Cell Biol.* 10, 45–51.
- Celis, J.E., Small, J.V., Larsen, P.M., Fey, S.J., De Mey, J., Celis, A., 1984. Intermediate filaments in monkey kidney TC7 cells: focal centers and interrelationship with other cytoskeletal systems. *Proc. Natl. Acad. Sci. USA* 81, 1117–1121.
- Chan, W.K., Yabe, J.T., Pimenta, A.F., Ortiz, D., Shea, T.B., 2003. Growth cones contain a dynamic population of neurofilament subunits. *Cell. Motil. Cytoskeleton* 54, 195–207.
- Correia, I., Chu, D., Chou, Y.H., Goldman, R.D., Matsudaira, P., 1999. Integrating the actin and vimentin cytoskeletons: adhesion-dependent formation of fimbrin-vimentin complexes in macrophages. *J. Cell Biol.* 146, 831–842.
- Coulombe, P.A., Wong, P., 2004. Cytoplasmic intermediate filaments revealed as dynamic and multipurpose scaffolds. *Nat. Cell Biol.* 6, 699–706.
- Fuchs, E., Karakesisoglou, I., 2001. Bridging cytoskeletal intersections. *Genes Dev.* 15, 1–14.
- Fujiwara, I., Takahashi, S., Tadakuma, H., Funatsu, T., Ishiwata, S., 2002. Microscopic analysis of polymerization dynamics with individual actin filaments. *Nat. Cell Biol.* 4, 666–673.
- Gard, D.L., Klymkowsky, M.W., 1998. Intermediate filament organization during oogenesis and early development in the clawed frog, *Xenopus laevis*. *Subcell. Biochem.* 31, 35–70.
- Gard, D.L., Cha, B.J., King, E., 1997. The organization and animal-vegetal asymmetry of cytokeratin filaments in stage VI *Xenopus* oocytes is dependent upon F-actin and microtubules. *Dev. Biol.* 184, 95–114.
- Goldman, R.D., 1971. The role of three cytoplasmic fibers in BHK-21 cell motility. I. Microtubules and the effects of colchicine. *J. Cell Biol.* 51, 752–762.
- Gordon III, W.E., Bushnell, A., Burrige, K., 1978. Characterization of the intermediate (10 nm) filaments of cultured cells using an autoimmune rabbit antiserum. *Cell* 13, 249–261.
- Gyoeva, F.K., Gelfand, V.I., 1991. Coalignment of vimentin intermediate filaments with microtubules depends on kinesin. *Nature* 353, 445–448.
- Hedberg, K.K., Chen, L.B., 1986. Absence of intermediate filaments in a human adrenal cortex carcinoma-derived cell line. *Exp. Cell Res.* 163, 509–517.
- Helfand, B.T., Mikami, A., Vallee, R.B., Goldman, R.D., 2002. A requirement for cytoplasmic dynein and dynactin in intermediate filament network assembly and organization. *J. Cell Biol.* 157, 795–806.
- Helfand, B.T., Chang, L., Goldman, R.D., 2003a. The dynamic and motile properties of intermediate filaments. *Annu. Rev. Cell Dev. Biol.* 19, 445–467.
- Helfand, B.T., Loomis, P., Yoon, M., Goldman, R.D., 2003b. Rapid transport of neural intermediate filament protein. *J. Cell Sci.* 116, 2345–2359.
- Helfand, B.T., Chang, L., Goldman, R.D., 2004. Intermediate filaments are dynamic and motile elements of cellular architecture. *J. Cell Sci.* 117, 133–141.
- Herrmann, H., Hesse, M., Reichenzeller, M., Aebi, U., Magin, T.M., 2003. Functional complexity of intermediate filament cytoskeletons: from structure to assembly to gene ablation. *Int. Rev. Cytol.* 223, 83–175.
- Hirokawa, N., 1998. Kinesin and dynein superfamily proteins and the mechanism of organelle transport. *Science* 279, 519–526.
- Hofmann, I., Franke, W.W., 1997. Heterotypic interactions and filament assembly of type I and type II cytokeratins in vitro: viscometry and determinations of relative affinities. *Eur. J. Cell Biol.* 72, 122–132.
- Hynes, R.O., Destree, A.T., 1978. 10 nm filaments in normal and transformed cells. *Cell* 13, 151–163.
- Knapp, L.W., O'Guin, W.M., Sawyer, R.H., 1983a. Rearrangement of the keratin cytoskeleton after combined treatment with microtubule and microfilament inhibitors. *J. Cell Biol.* 97, 1788–1794.

- Knapp, L.W., O'Guin, W.M., Sawyer, R.H., 1983b. Drug-induced alterations of cytokeratin organization in cultured epithelial cells. *Science* 219, 501–503.
- Kreitzer, G., Liao, G., Gundersen, G.G., 1999. Detyrosination of tubulin regulates the interaction of intermediate filaments with microtubules in vivo via a kinesin-dependent mechanism. *Mol. Biol. Cell* 10, 1105–1118.
- Leung, C.L., Green, K.J., Liem, R.K., 2002. Plakins: a family of versatile cytolinker proteins. *Trends Cell Biol.* 12, 37–45.
- Liao, G., Gundersen, G.G., 1998. Kinesin is a candidate for cross-bridging microtubules and intermediate filaments. Selective binding of kinesin to detyrosinated tubulin and vimentin. *J. Biol. Chem.* 273, 9797–9803.
- Liovic, M., Mogensen, M.M., Prescott, A.R., Lane, E.B., 2003. Observation of keratin particles showing fast bidirectional movement colocalized with microtubules. *J. Cell Sci.* 116, 1417–1427.
- Martys, J.L., Ho, C.L., Liem, R.K., Gundersen, G.G., 1999. Intermediate filaments in motion: observations of intermediate filaments in cells using green fluorescent protein-vimentin. *Mol. Biol. Cell* 10, 1289–1295.
- Osborn, M., Franke, W.W., Weber, K., 1977. Visualization of a system of filaments 7–10 nm thick in cultured cells of an epithelioid line (Pt K2) by immunofluorescence microscopy. *Proc. Natl. Acad. Sci. USA* 74, 2490–2494.
- Osborn, M., Franke, W., Weber, K., 1980. Direct demonstration of the presence of two immunologically distinct intermediate-sized filament systems in the same cell by double immunofluorescence microscopy. Vimentin and cytokeratin fibers in cultured epithelial cells. *Exp. Cell Res.* 125, 37–46.
- Pollard, T.D., Borisy, G.G., 2003. Cellular motility driven by assembly and disassembly of actin filaments. *Cell* 112, 453–465.
- Prahlad, V., Yoon, M., Moir, R.D., Vale, R.D., Goldman, R.D., 1998. Rapid movements of vimentin on microtubule tracks: kinesin-dependent assembly of intermediate filament networks. *J. Cell Biol.* 143, 159–170.
- Prahlad, V., Helfand, B.T., Langford, G.M., Vale, R.D., Goldman, R.D., 2000. Fast transport of neurofilament protein along microtubules in squid axoplasm. *J. Cell Sci.* 113, 3939–3946.
- Rao, M.V., Engle, L.J., Mohan, P.S., Yuan, A., Qiu, D., Cataldo, A., Hassinger, L., Jacobsen, S., Lee, V.M., Andreadis, A., Julien, J.P., Bridgman, P.C., Nixon, R.A., 2002. Myosin Va binding to neurofilaments is essential for correct myosin Va distribution and transport and neurofilament density. *J. Cell Biol.* 159, 279–290.
- Rottner, K., Behrendt, B., Small, J.V., Wehland, J., 1999. VASP dynamics during lamellipodia protrusion. *Nat. Cell Biol.* 1, 321–322.
- Roy, S., Coffee, P., Smith, G., Liem, R.K., Brady, S.T., Black, M.M., 2000. Neurofilaments are transported rapidly but intermittently in axons: implications for slow axonal transport. *J. Neurosci.* 20, 6849–6861.
- Shah, J.V., Flanagan, L.A., Janmey, P.A., Leterrier, J.F., 2000. Bidirectional translocation of neurofilaments along microtubules mediated in part by dynein/dynactin. *Mol. Biol. Cell* 11, 3495–3508.
- Steinbock, F.A., Wiche, G., 1999. Plectin: a cytolinker by design. *Biol. Chem.* 380, 151–158.
- Strnad, P., Windoffer, R., Leube, R.E., 2001. In vivo detection of cytokeratin filament network breakdown in cells treated with the phosphatase inhibitor okadaic acid. *Cell Tissue Res.* 306, 277–293.
- Strnad, P., Windoffer, R., Leube, R.E., 2002. Induction of rapid and reversible cytokeratin filament network remodeling by inhibition of tyrosine phosphatases. *J. Cell Sci.* 115, 4133–4148.
- Strnad, P., Windoffer, R., Leube, R.E., 2003. Light-induced resistance of the keratin network to the filament-disrupting tyrosine phosphatase inhibitor orthovanadate. *J. Invest. Dermatol.* 120, 198–203.
- Sun, T.T., Green, H., 1978. Immunofluorescent staining of keratin fibers in cultured cells. *Cell* 14, 469–476.
- Tint, I.S., Hollenbeck, P.J., Verkhovskiy, A.B., Surgucheva, I.G., Bershadsky, A.D., 1991. Evidence that intermediate filament reorganization is induced by ATP-dependent contraction of the actomyosin cortex in permeabilized fibroblasts. *J. Cell Sci.* 98, 375–384.
- Vasioukhin, V., Bauer, C., Yin, M., Fuchs, E., 2000. Directed actin polymerization is the driving force for epithelial cell–cell adhesion. *Cell* 100, 209–219.
- Wang, L., Brown, A., 2001. Rapid intermittent movement of axonal neurofilaments observed by fluorescence photobleaching. *Mol. Biol. Cell* 12, 3257–3267.
- Wang, L., Ho, C.L., Sun, D., Liem, R.K., Brown, A., 2000. Rapid movement of axonal neurofilaments interrupted by prolonged pauses. *Nat. Cell Biol.* 2, 137–141.
- Waterman-Storer, C.M., Salmon, E.D., 1997. Actomyosin-based retrograde flow of microtubules in the lamella of migrating epithelial cells influences microtubule dynamic instability and turnover and is associated with microtubule breakage and treadmilling. *J. Cell Biol.* 139, 417–434.
- Weber, K.L., Bement, W.M., 2002. F-actin serves as a template for cytokeratin organization in cell free extracts. *J. Cell Sci.* 115, 1373–1382.
- Werner, N.S., Windoffer, R., Strnad, P., Grund, C., Leube, R.E., Magin, T.M., 2004. Epidermolysis bullosa simplex-type mutations alter the dynamics of the keratin cytoskeleton and reveal a contribution of actin to the transport of keratin subunits. *Mol. Biol. Cell* 15, 990–1002.
- Wiche, G., 1998. Role of plectin in cytoskeleton organization and dynamics. *J. Cell Sci.* 111, 2477–2486.
- Windoffer, R., Leube, R.E., 1999. Detection of cytokeratin dynamics by time-lapse fluorescence microscopy in living cells. *J. Cell Sci.* 112, 4521–4534.
- Windoffer, R., Leube, R.E., 2001. De novo formation of cytokeratin filament networks originates from the cell cortex in A-431 cells. *Cell Motil. Cytoskeleton* 50, 33–44.
- Windoffer, R., Leube, R.E., 2004. Imaging of keratin dynamics during the cell cycle and in response to phosphatase inhibition. *Methods Cell Biol.* 78, 321–352.
- Windoffer, R., Borchert-Stuhltrager, M., Leube, R.E., 2002. Desmosomes: interconnected calcium-dependent structures of remarkable stability with significant integral membrane protein turnover. *J. Cell Sci.* 115, 1717–1732.
- Windoffer, R., Woll, S., Strnad, P., Leube, R.E., 2004. Identification of novel principles of keratin filament network turnover in living cells. *Mol. Biol. Cell* 15, 2436–2448.

- Xia, C.H., Roberts, E.A., Her, L.S., Liu, X., Williams, D.S., Cleveland, D.W., Goldstein, L.S., 2003. Abnormal neurofilament transport caused by targeted disruption of neuronal kinesin heavy chain KIF5A. *J. Cell Biol.* 161, 55–66.
- Yabe, J.T., Pimenta, A., Shea, T.B., 1999. Kinesin-mediated transport of neurofilament protein oligomers in growing axons. *J. Cell Sci.* 112, 3799–3814.
- Yabe, J.T., Jung, C., Chan, W.K., Shea, T.B., 2000. Phospho-dependent association of neurofilament proteins with kinesin in situ. *Cell Motil. Cytoskeleton* 45, 249–262.
- Yabe, J.T., Chan, W.K., Chylinski, T.M., Lee, S., Pimenta, A.F., Shea, T.B., 2001. The predominant form in which neurofilament subunits undergo axonal transport varies during axonal initiation, elongation, and maturation. *Cell Motil. Cytoskeleton* 48, 61–83.
- Yoon, M., Moir, R.D., Prahlad, V., Goldman, R.D., 1998. Motile properties of vimentin intermediate filament networks in living cells. *J. Cell Biol.* 143, 147–157.
- Yoon, K.H., Yoon, M., Moir, R.D., Khuon, S., Flitney, F.W., Goldman, R.D., 2001. Insights into the dynamic properties of keratin intermediate filaments in living epithelial cells. *J. Cell Biol.* 153, 503–516.
- Zaidel-Bar, R., Ballestrem, C., Kam, Z., Geiger, B., 2003. Early molecular events in the assembly of matrix adhesions at the leading edge of migrating cells. *J. Cell Sci.* 116, 4605–4613.